High-Resolution Neutron Diffraction Monochromators for Neutron Diffractometry

Pavol Mikula,
Nuclear Physics Institute ASCR
250 68 Řež near Prague, Czech Republic

NMI3-Meeting, Barcelona, 2010

Motivation

- **Backscattering setting can be easily realized for a rather small take-off angle of the monochromator.**
- **Monochromatic beam is highly collimated.**
- **$\Delta\lambda$ -spread depends on the effective mosaicity of both reflections participating on the double dif-fraction process ($\Delta\lambda/\lambda$ is about 10^{-3} or less). No Soller collimators are required. If necessary, beam can be defined by slits.**

Therefore

- **Further studies of multiple reflections (MR) in bent perfect crystals**
- **To identify strong MR effects for possible applications in high resolution diffractometry**
- **To construct testing multipurpose diffractometer employing MR monochromator**
- **Testing of new ideas and diffractometer arrangements, where MR-monochromators or MR-analyzers are employed**
- **MC simulations of MR-effects which have not been carried out**

Neutron optics testing bench

Fixed take off angle
of the premonochromator

$\lambda = 0.1629\ \text{nm} \pm \Delta\lambda$

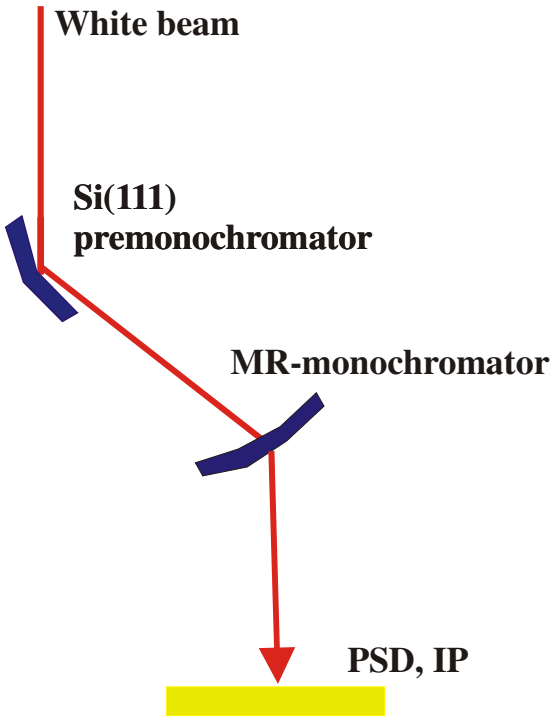

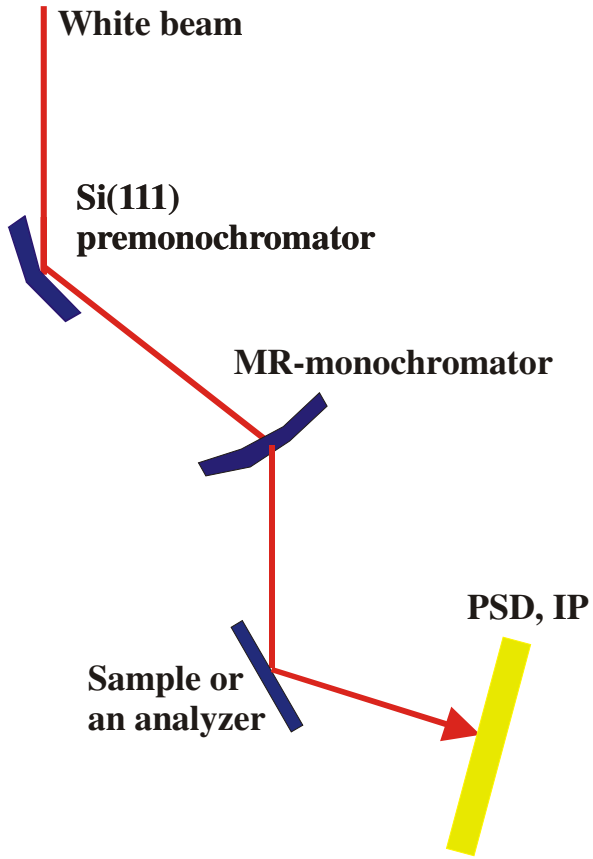

MR-monochromators - Si(222), Si(002) or Ge(222), Ge(002) set for diffraction in symmetric or asymmetric transmission/reflection geometry

Multiple-reflection (MR) monochromator

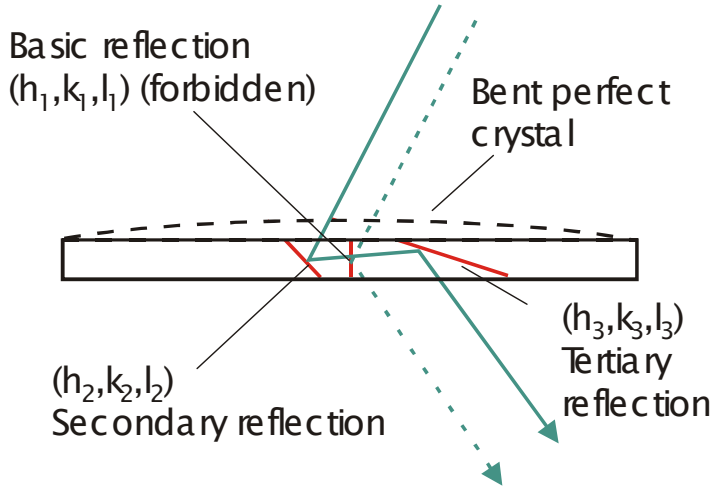

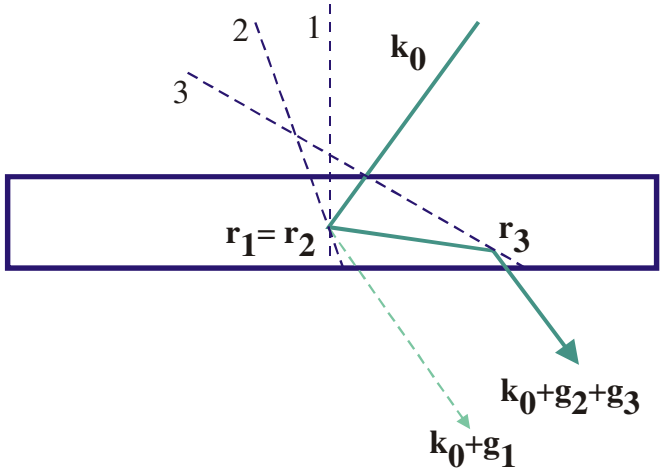

$$\vec{g}_1 = \vec{g}_2 + \vec{g}_3$$

Relation for scattering vectors

Double reflection realized on (h_2,k_2,l_2) and (h_3,k_3,l_3) in a bent perfect or mosaic single crystal can simulate a forbidden primary reflection (or strengthen a week one) corresponding to (h_1,k_1,l_1). Due to the bending the double reflection reflectivity can be substantially increased that such a monochromator crystal can provide a good intensity of highly monochromatic and highly collimated beam for a further use.

Search for multiple reflections in a single crystal

Momentum space representation of a multiple reflection process

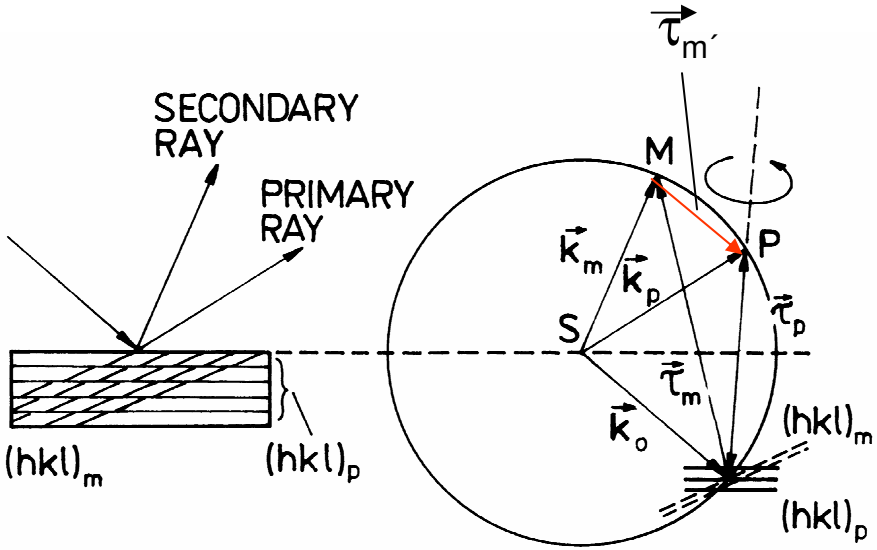

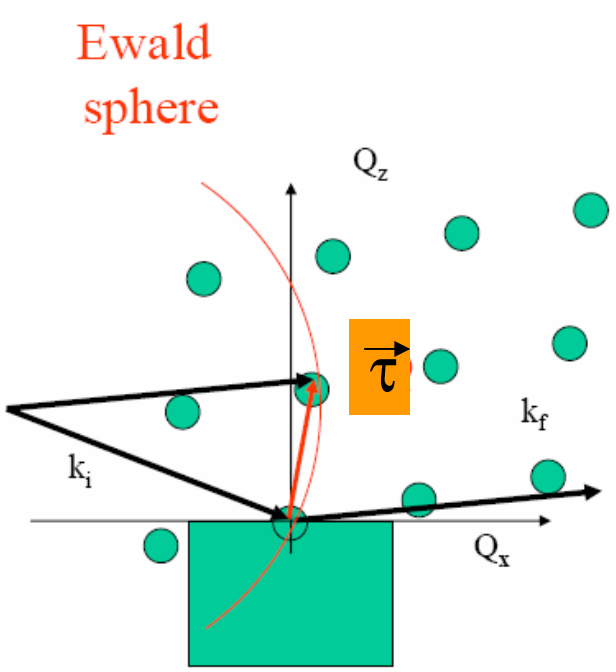

Relation for scattering vectors $\Longrightarrow \quad \vec{\tau}_p = \vec{\tau}_m + \vec{\tau}_{m'}$

In the search of strong multiple reflection effects two methods are usually used:

a. The method of azimuthal rotation of the crystal lattice around the scattering vector of the primary reflection for a fixed wavelength.

b. The method of θ–$2\theta_D$ scan in the white beam for a fixed azimuthal angle.

Search for strong multiple-reflection effects

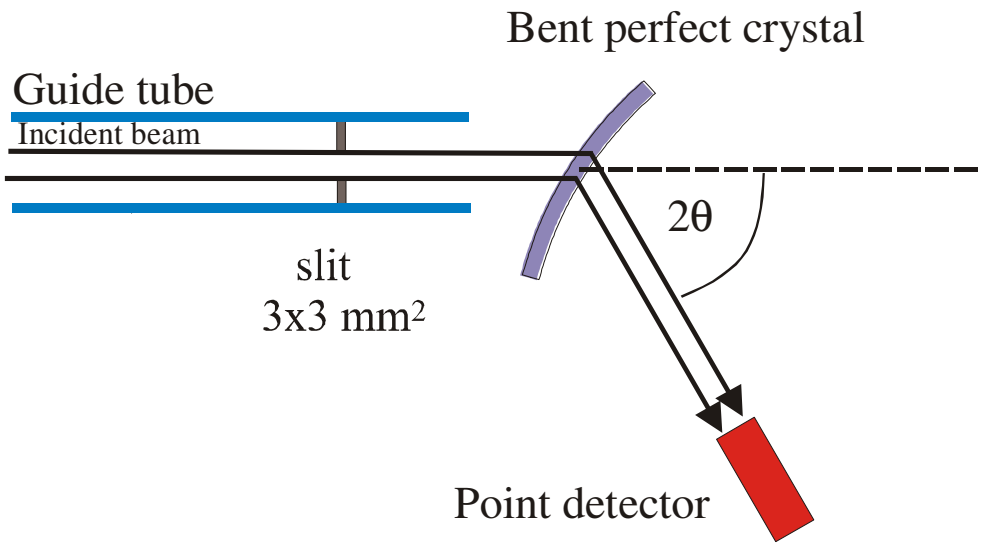

For the experimental search of strong multiple reflection effects we used three Si slabs of different cut.

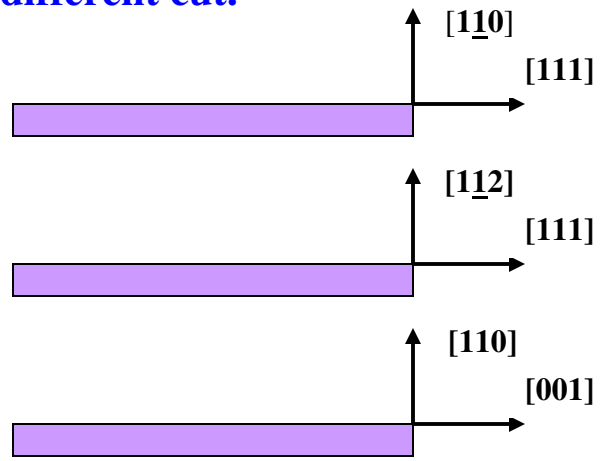

Experimental arrangement with symmetric transmission geometry of the bent perfect Si crystal as used for an identification of umweg-reflections by θ–2θ scanning.

Thanks to symmetric transmission geometry, crystal deformation has no influence on the reflectivity related to the basic primary reflection and its higher orders. This is not valid for mosaic crystals.

Search for strong multiple-reflection effects

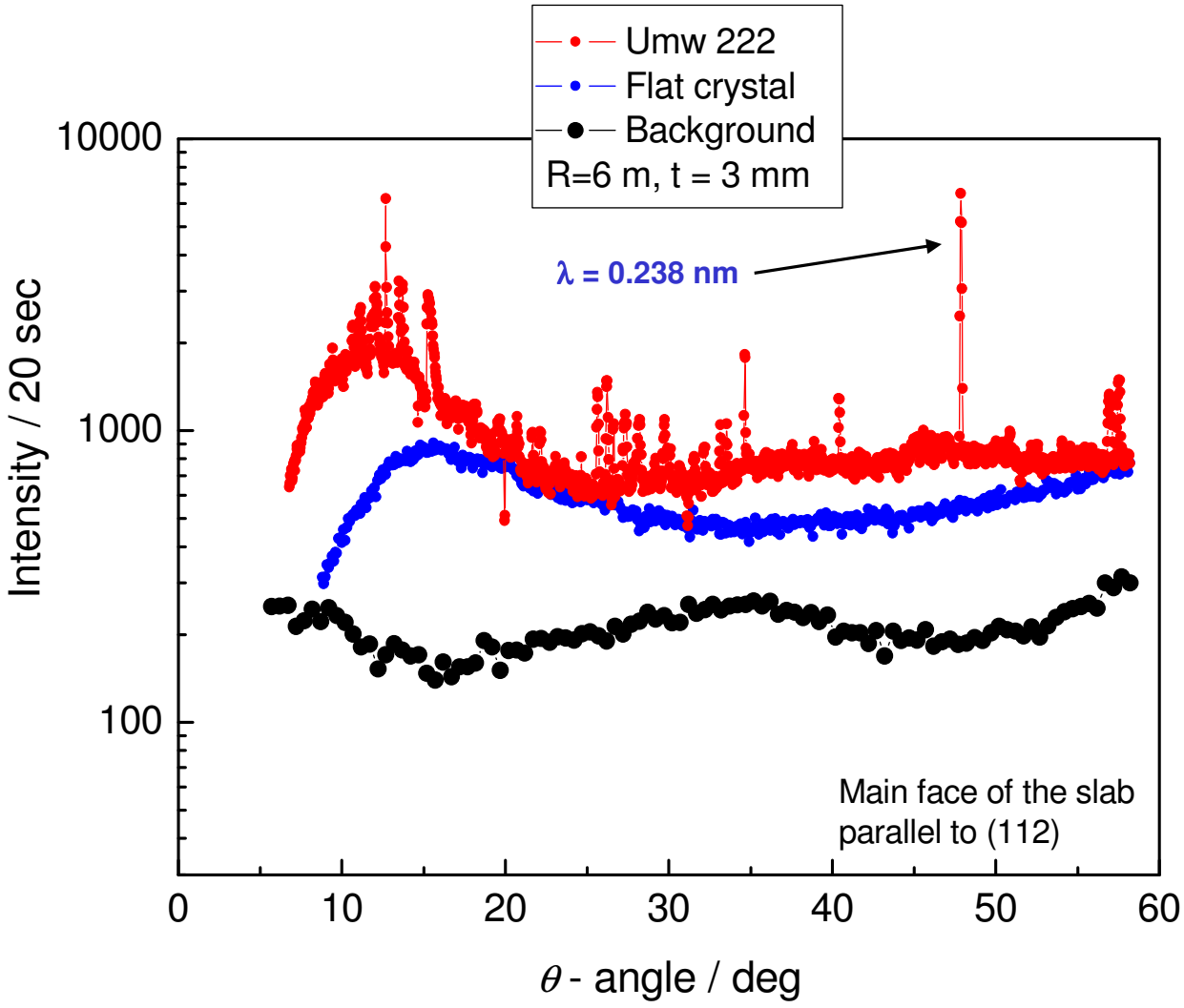

θ–2θ scan taken with the Si crystal slab set for 222 forbidden reflection in symmetric transmission geometry.

Multiple reflection monochromator

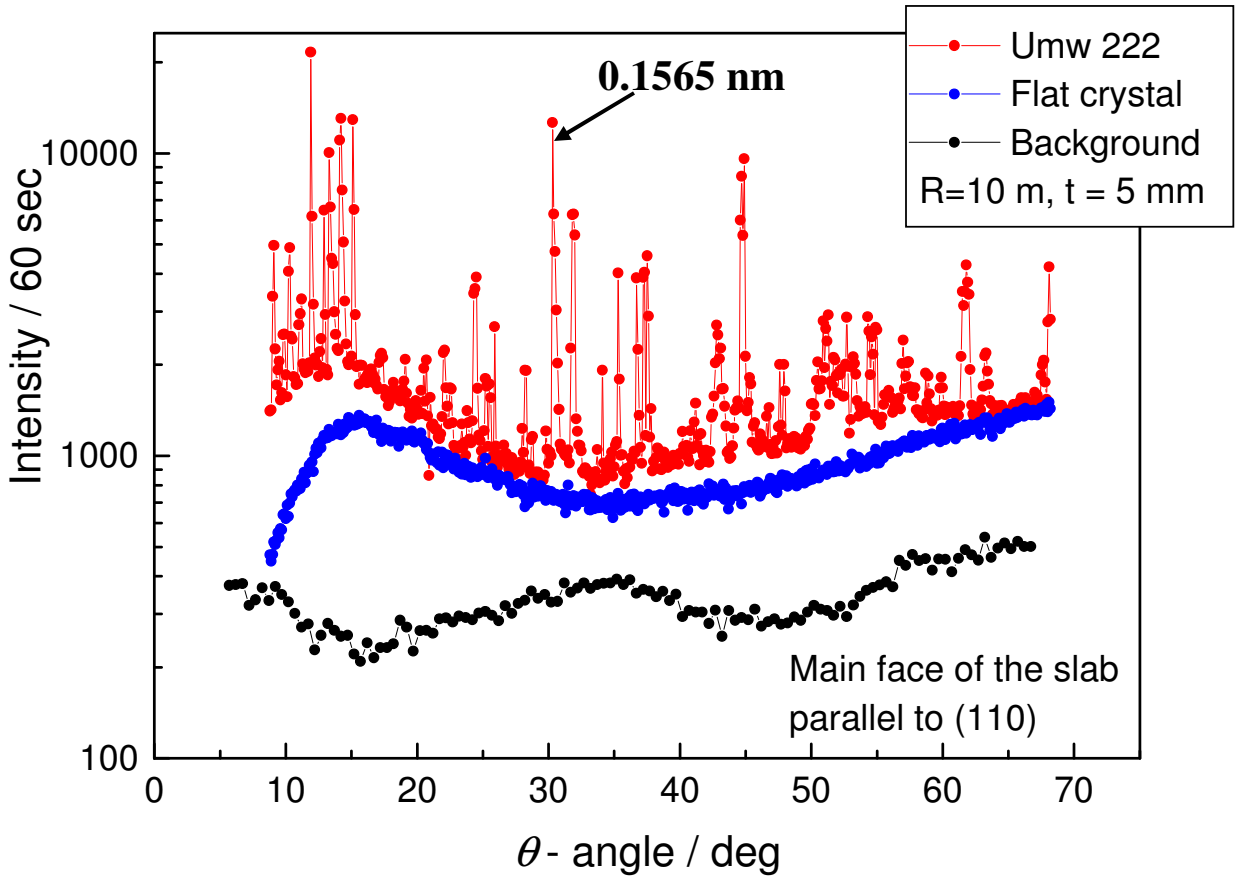

θ–2θ scan taken with the Si(222) crystal slab set for diffraction in symmetric transmission geometry; if we use Ge(222) slab the corresponding wavelength is 0.1629 nm.

Search for strong multiple-reflection effects

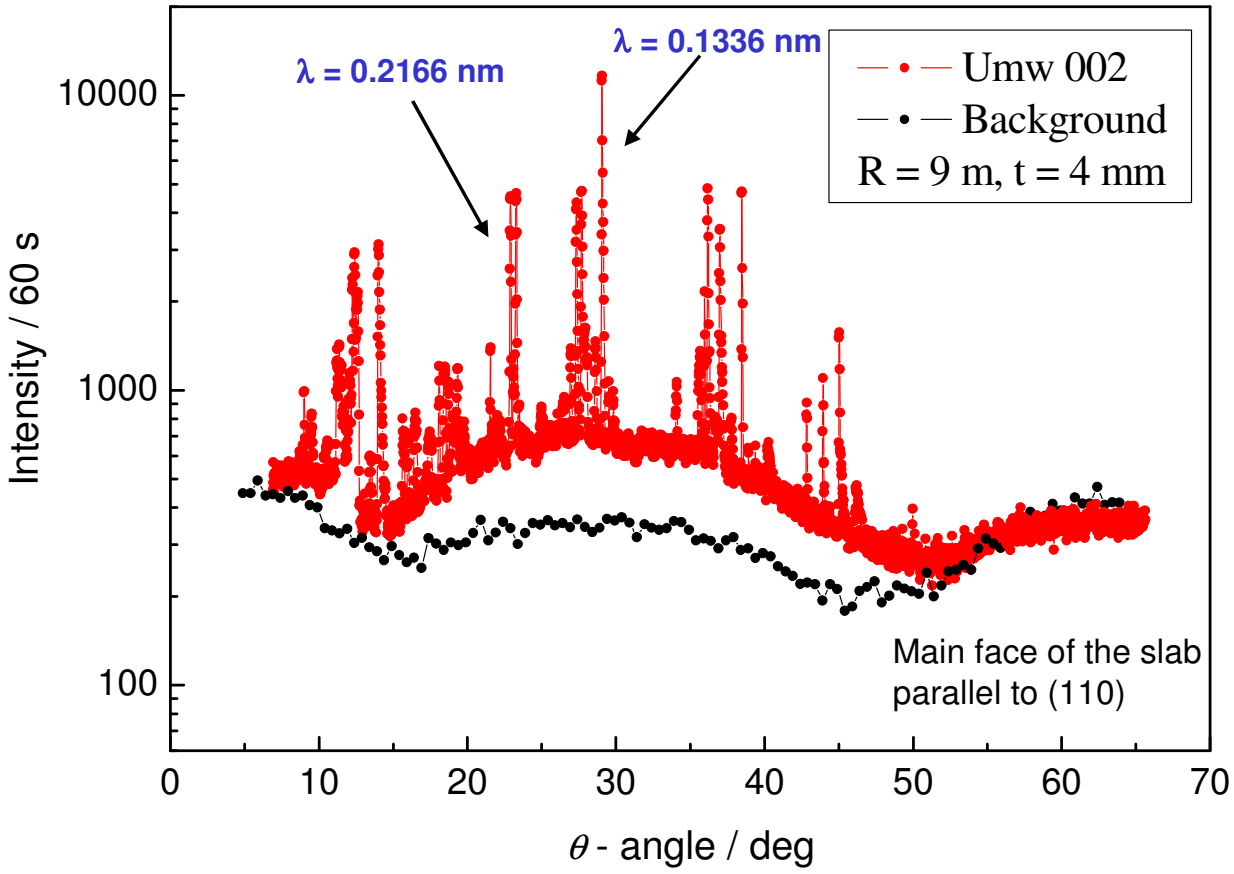

θ–2θ scan taken with the Si crystal slab set for 002 forbidden reflection in symmetric transmission geometry

Test of the beam divergence at λ=0.2348 nm

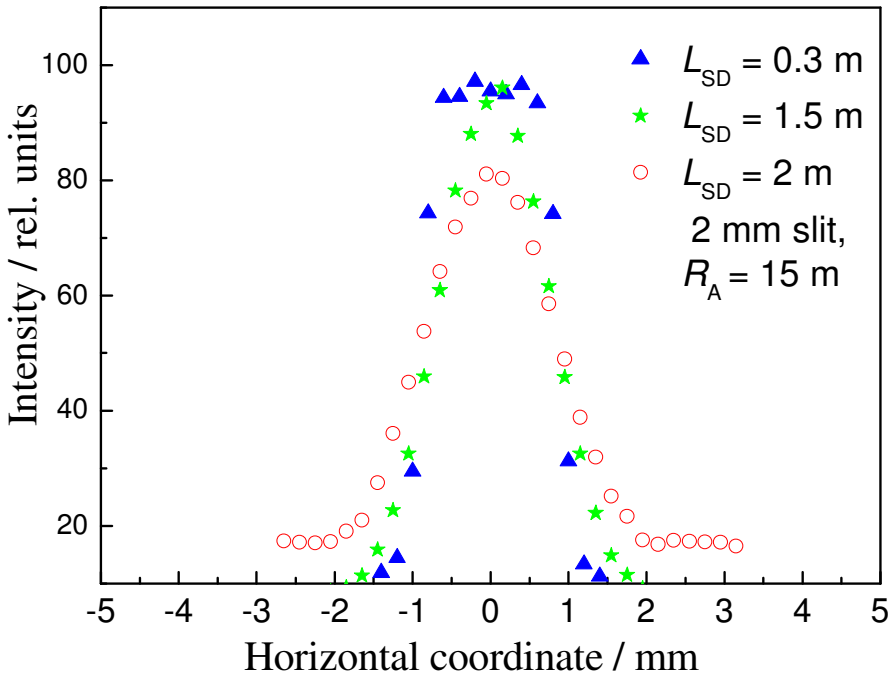

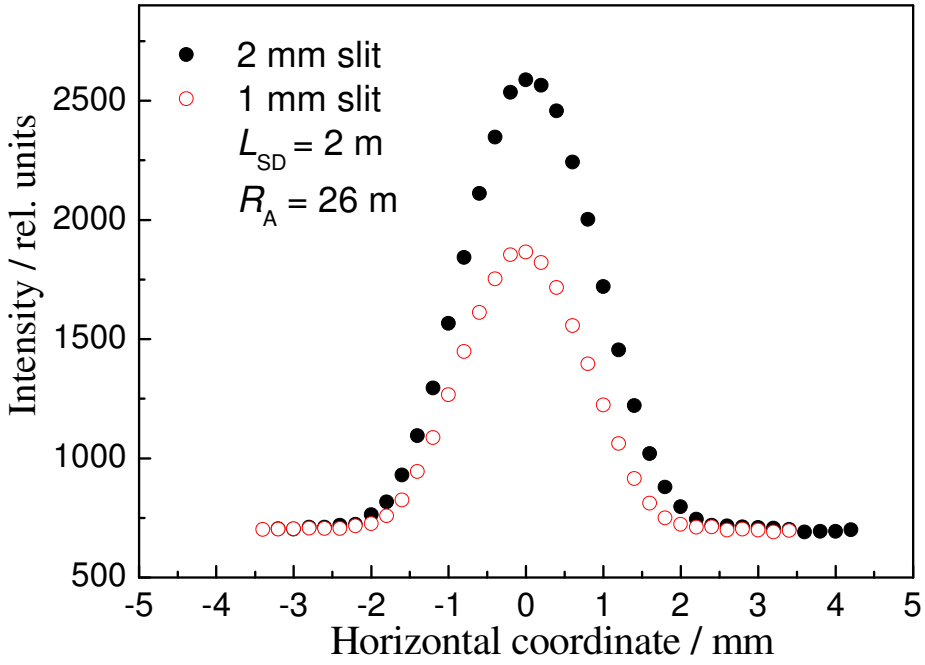

FWHM is in this case determined by the spatial resolution of the PSD

Images of the obtained beam profiles (intensity distribution on the horizontal scale) taken by 1d-PSD. L_{SD} – the distance between the bent crystal and the PSD.

Examples of the α-Fe powder diffraction profiles taken with the Si(222) mutiple-reflection monochromator

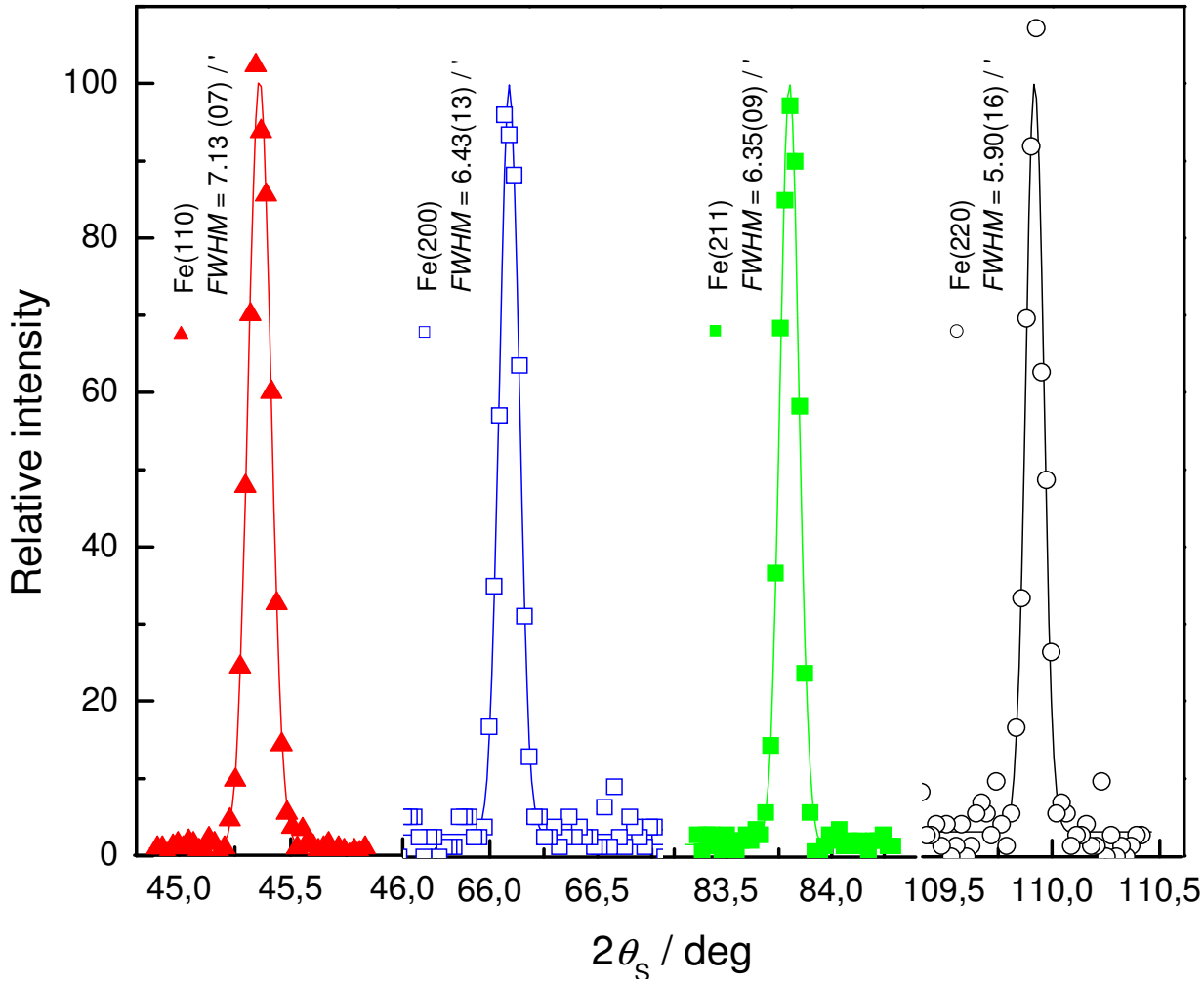

λ = 0.1565 nm

The obtained *FWHM* is determined by the width of the sample (Φ=2 mm) and the spatial resolution of the PSD (1.5 mm)

No Soller collimators!!!

Experimental test with a multiphase steel sample

The high-resolution diffraction performance we used for investigation of Fe-reflections in an induction hardened S45C rod (Φ=20 mm) having different phase composition at different distances from the rod axis. For determination of gauge volume we used 2 mm input and output slits in the incident as well as diffracted beam, respectively.

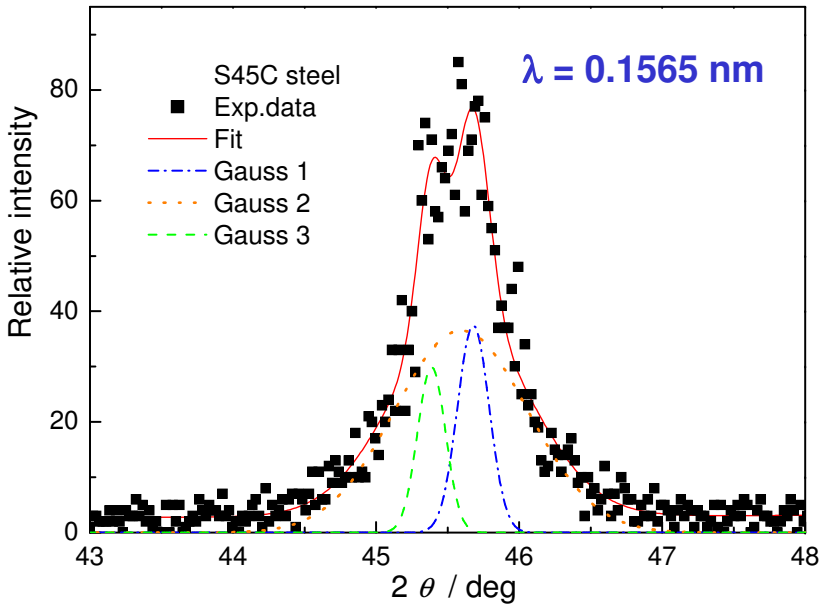

Induction-hardened S45C steel diffraction profile taken at 2 mm under the surface with the fitted profiles corresponding to the perlitic, ferritic and martensitic phases.

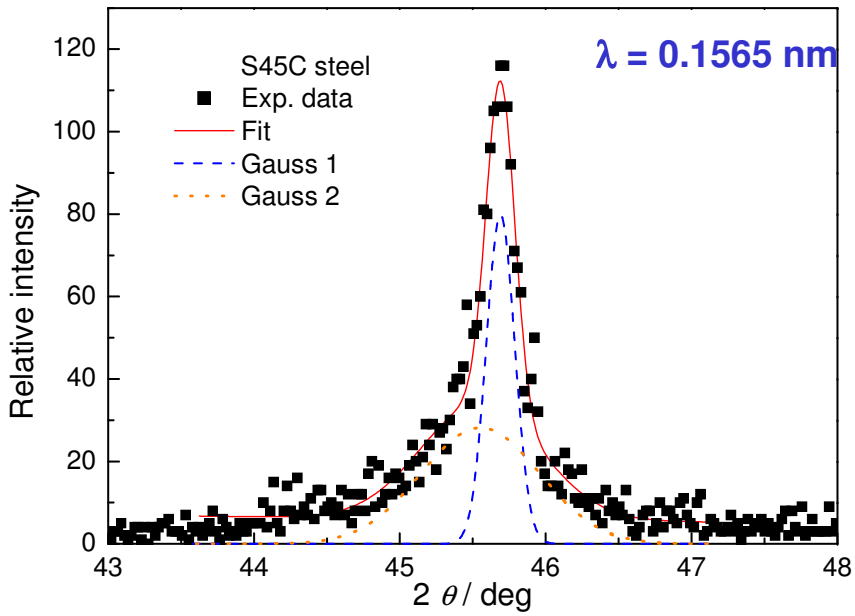

Induction-hardened S45C steel diffraction profile taken at 4 mm under the surface with the fitted profiles corresponding to the ferritic and martensitic phases.

Experimental high-resolution neutron radiography tests

In addition to a possibility of using a highly collimated beam for conventional absorption radiography with a imaging plate at a rather large distance from the sample, highly collimated neutrons obtained by means of dispersive multiple reflection monochromator can be considered as plane waves and permit to design a completely new technique of phase contrast neutron radiography experiments at a distance much smaller in comparison with the conventional pin-hole geometry. The folloving preliminary tests on office staples at $\lambda = 0.238$ nm have been carried out with the imaging plate situated at the distance of 70 cm from the sample.

First neutron radiography tests

Screw

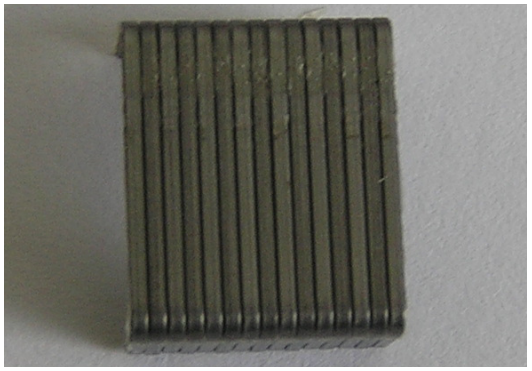

Office staples

λ = 0.238 nm

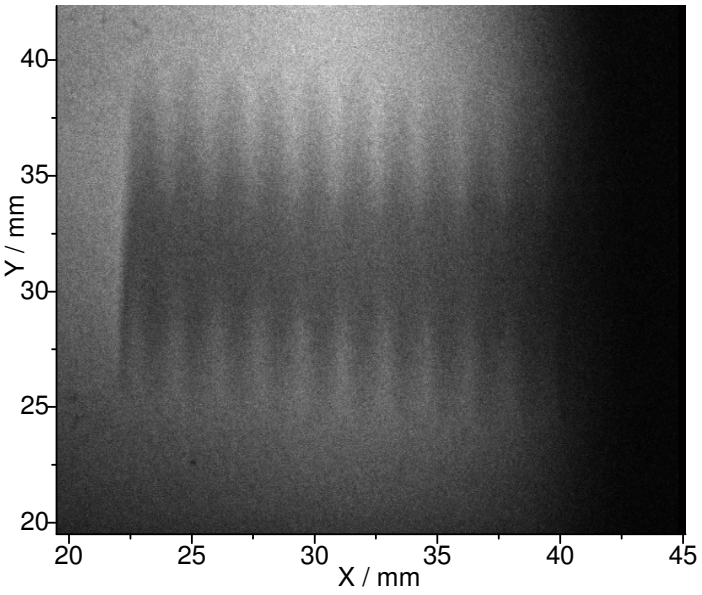

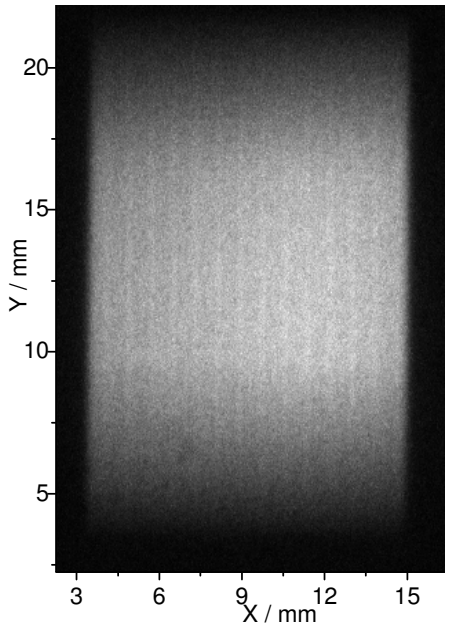

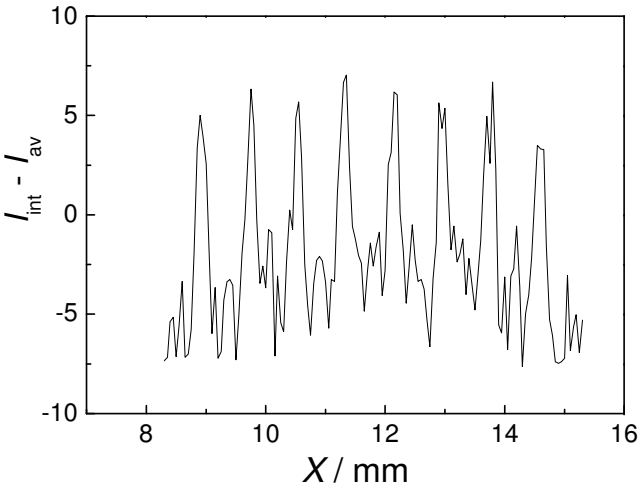

Radiography tests at λ = 0.165 nm

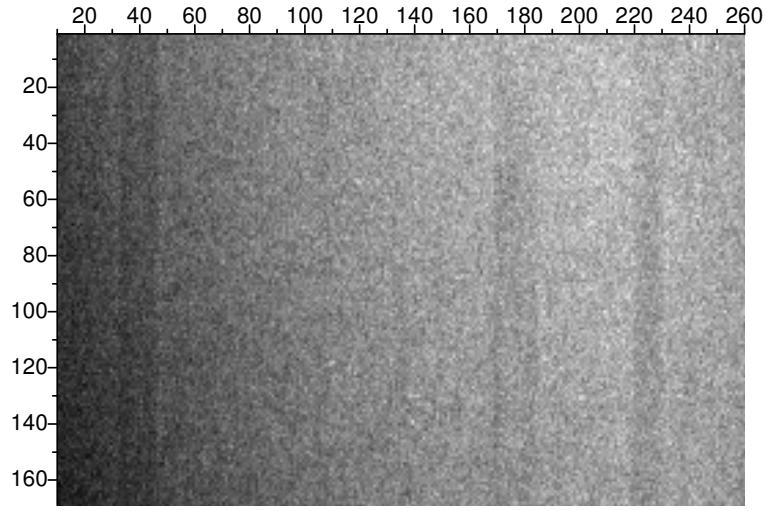

Neutron radiography of the office staple (1), Cu-wire (2), hair (3), needle- grouting point (4), graphite–black lead (5). X-Y: Pixel numbers, spatial resolution 50 µm – 1 pixel.

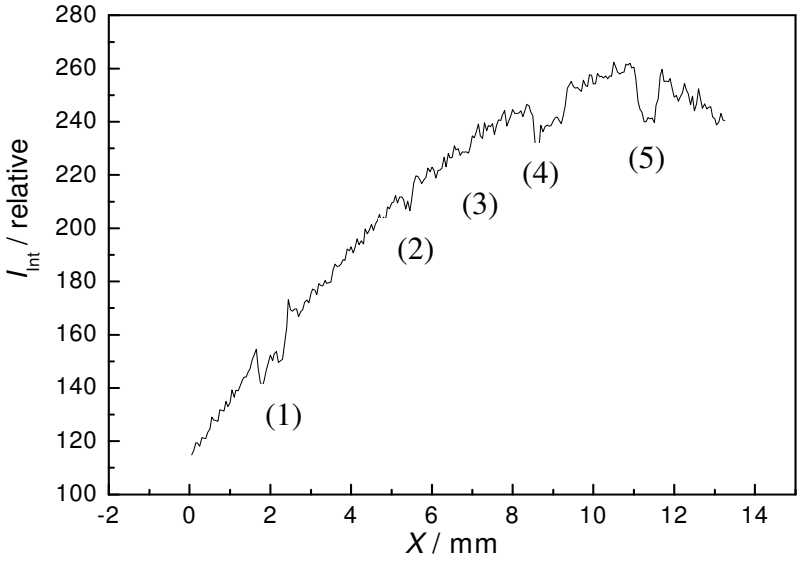

Intensity data integrated in the Y-direction

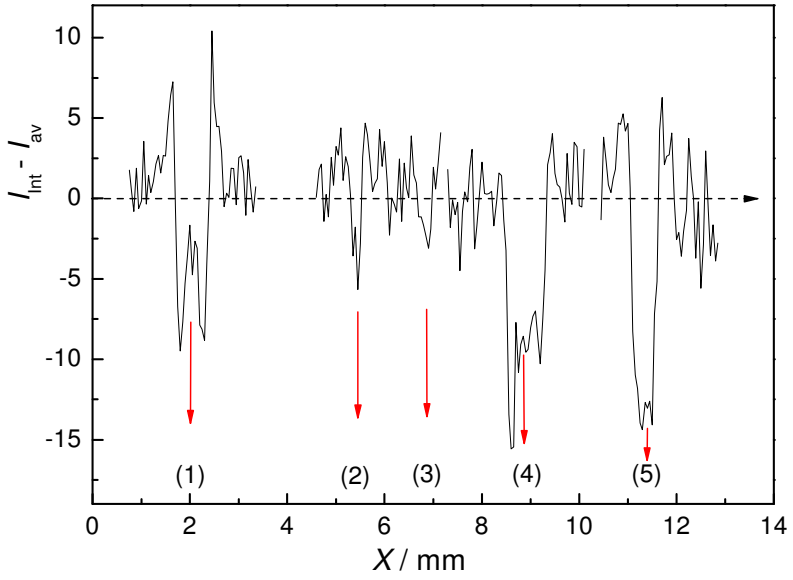

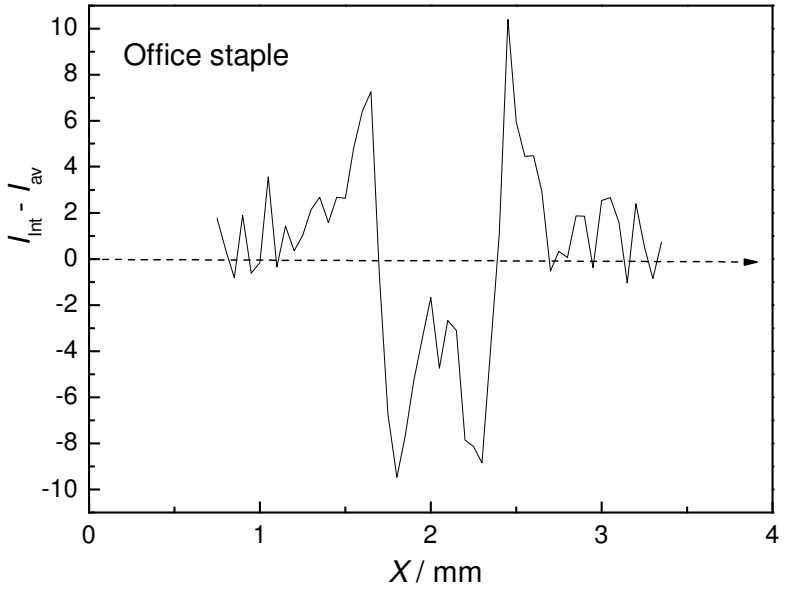

Intensity distribution in the vicinity of the image of the chosen samples

New investigations

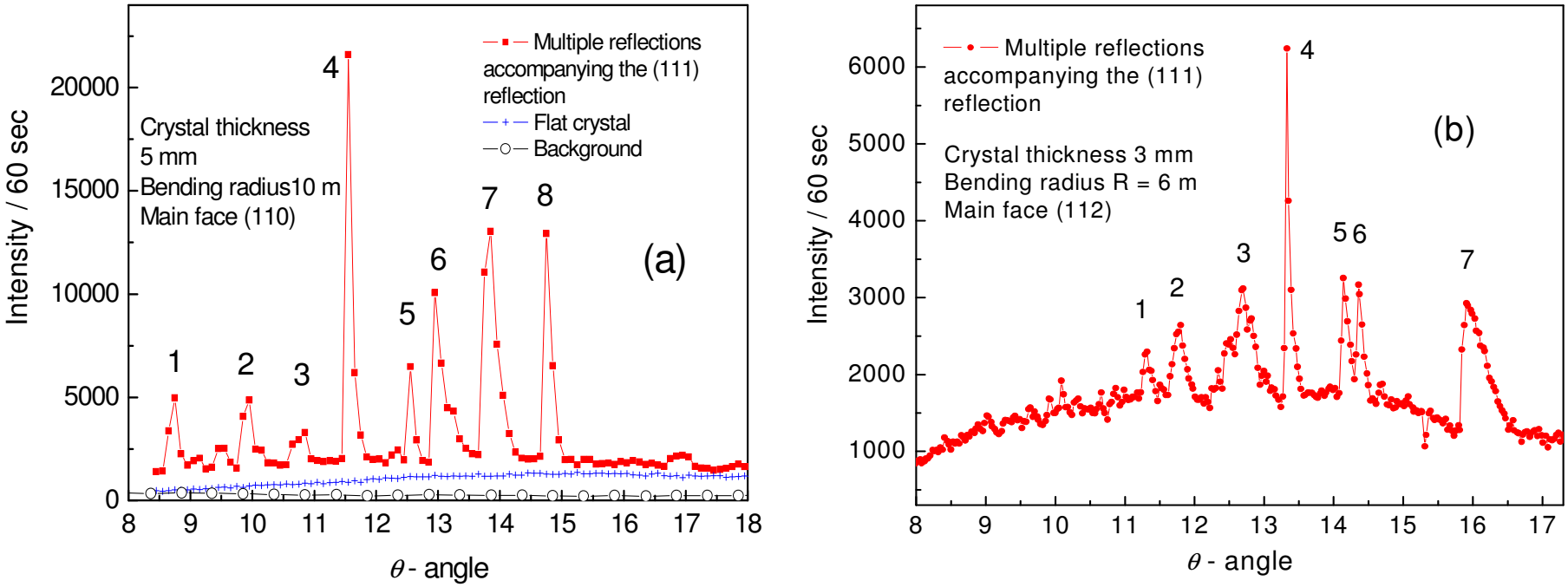

Enlarged parts of the θ-2θ scans where strong multiple reflections accompanying the allowed 111 reflection were observed

P. Mikula, M. Vrána, J. Šaroun, B.S. Seong, V. Em and M.K. Moon, *Multiple neutron Bragg reflections in single crystals should not be considered negligible*, In the Proc. of Int. Workshop on Neutron Optics NOP2010, Alpe d'Huez near Grenoble, France, 17-19th of March 2010, submitted to NIM.

Peak N.	Primary, secondary and tertiary reflections	Wavelength /Å	Bragg angle /deg
1a	111/315/404	0.948	8.704
1a	111/153/044	0.948	8.704
1a	111/311/422	0.948	8.704
1a	111/404/513	0.948	8.704
1a	111/044/135	0.948	8.704
1a	111/242/131	0.948	8.704
2a	111/224/315	1.08	9.924
2a	111/135/224	1.08	9.924
3a	111/355/444	1.16	10.67
3a	111/444/535	1.16	10.67
4a	111/313/404	1.253	11.536
4a	111/044/133	1.253	11.536
4a	111/133/022	1.253	11.536
4a	111/202/313	1.253	11.536
5a	111/353/444	1.362	12.553
5a	111/444/533	1.362	12.553
6a	111/511/602	1.403	12.993
6a	111/062/151	1.403	12.993
7a	111/133/224	0.1492	13.763
7a	111/151/040	0.1492	13.763
7a	111/400/511	0.1492	13.763
7a	111/224/313	0.1492	13.763
8a	111/153/242	0.1592	14.705
8a	111/422/513	0.1592	14.705

Peak N.	Primary, secondary and tertiary reflections	Wavelength /Å	Bragg angle /deg
1b	111/135/224	1.241	11.421
1b	111/315/224	1.241	11.421
2b	111/533/642	1.266	11.653
2b	111/353/462	1.266	11.653
3b	111/117/206	1.376	12.679
3b	111/117/026	1.376	12.679
3b	111/317/426	1.389	12.804
3b	111/137/246	1.389	12.804
3b	111/246/355	1.389	12.804
3b	111/426/535	1.389	12.804
4b	111/311/400	1.438	13.262
4b	111/131/040	1.438	13.262
4b	111/331/440	1.438	13.262
4b	111/220/331	1.438	13.262
5b	111/242/351	1.535	14.173
6b	111/335/444	1.561	14.420
7b	111/224/313	1.706	15.793
7b	111/224/133	1.706	15.793

Calculated parameters related to the peaks accompanying 111 reflections for two different cuts of the slab

Monte Carlo simulations of parasitic and multiple Bragg reflections

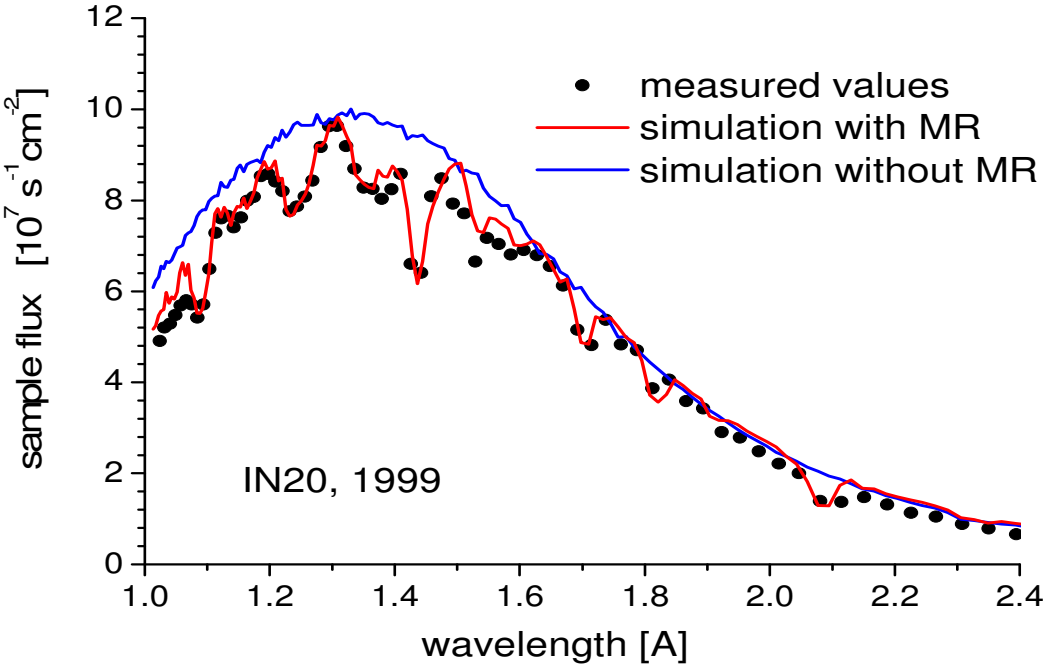

Comparison of measured in 1999 and simulated monochromatic flux at IN20.
Experimental data from
J. Saroun, J. Kulda, A. Wildes, A. Hiess, Physica B 276-278 (2000) 148.

- A new ray-tracing code has been developed, which permits **quantitative predictions of the intensities of parasitic and multiple reflections** (U*mweganregung*) in elasticaly bent perfect crystals including
- Good **agreement with experimental data**
- Part of the next RESTRAX release - **available for instrument development**: *prediction of monochromatic flux, filterig properties, new monochromator and analyzers ...*

Comparison with experiment - Umweganregung

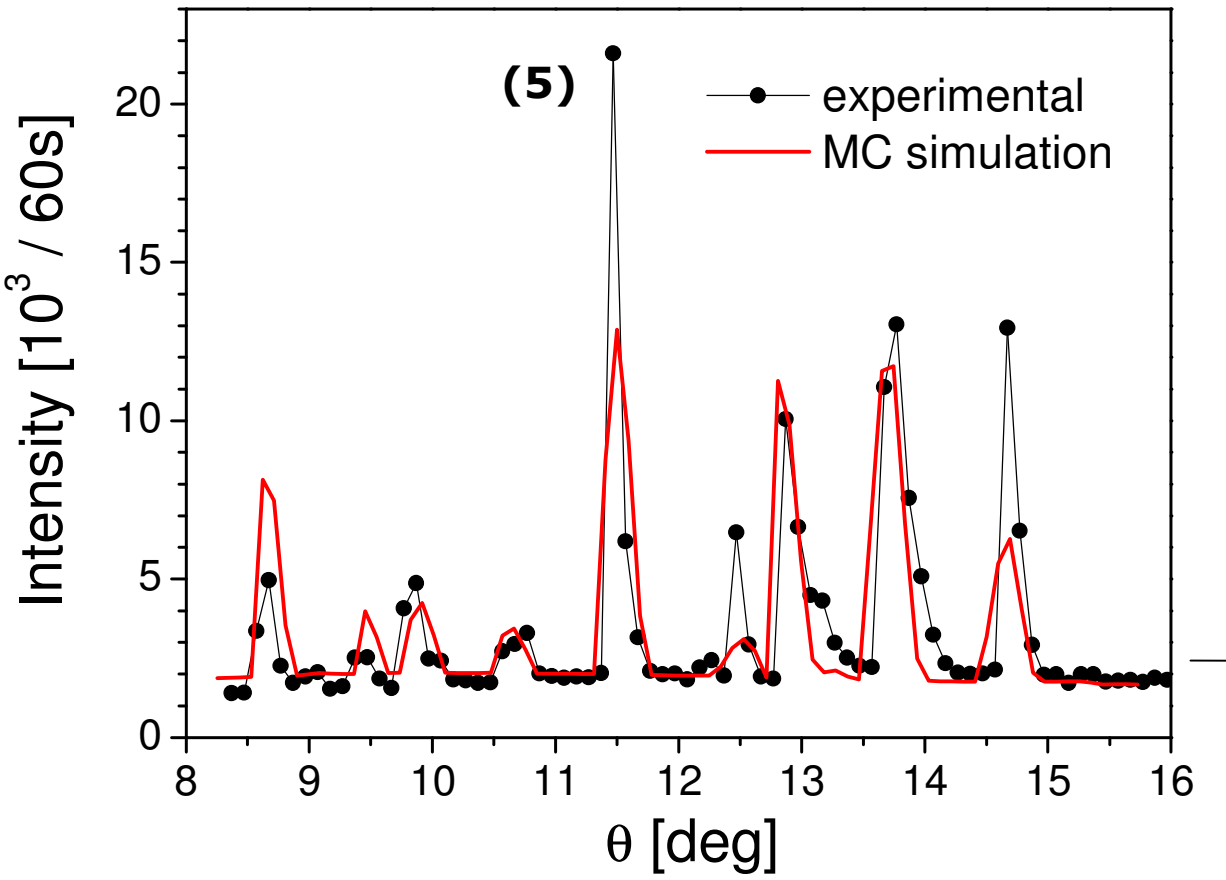

peak (5)

313 + 404 = 111
044 + 133 = 111
133 + 022 = 111
202 + 313 = 111

Measurement: POLDI, GKSS Geesthacht, **MC simulation:** RESTRAX ver. 6.0.8

J. Šaroun, P. Mikula, J. Kulda, *Monte Carlo simulations of parasitic and multiple reflections in elastically bent perfect single-crystals*, In the Proc. of Int. Workshop on Neutron Optics NOP2010, Alpe d'Huez near Grenoble, France, 17-19th of March 2010, submitted to NIM.

Application: Multianalyzer systems in transmission arrangement

Simulated setup - SIMRES

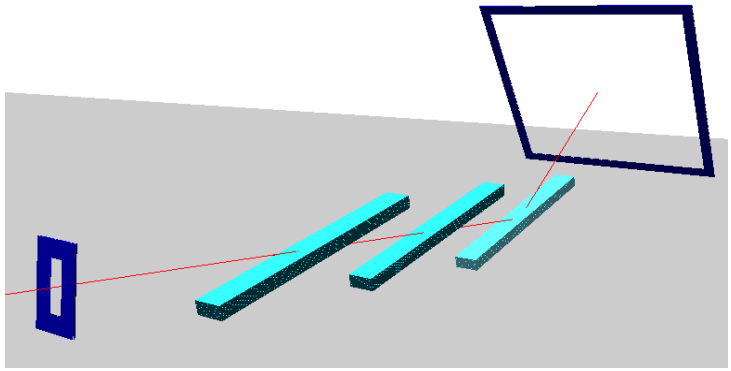

source (sample)
5 x 20 mm^2, isotropic, uniform spectrum
distance=150 cm

crystals
20 x 200 mm, 10 x 1 mm sandwich
monochromatic focusing to the source
mutual angle $\Delta\theta$ **=1.5°**
~ channel of a flatcone multianalyzer

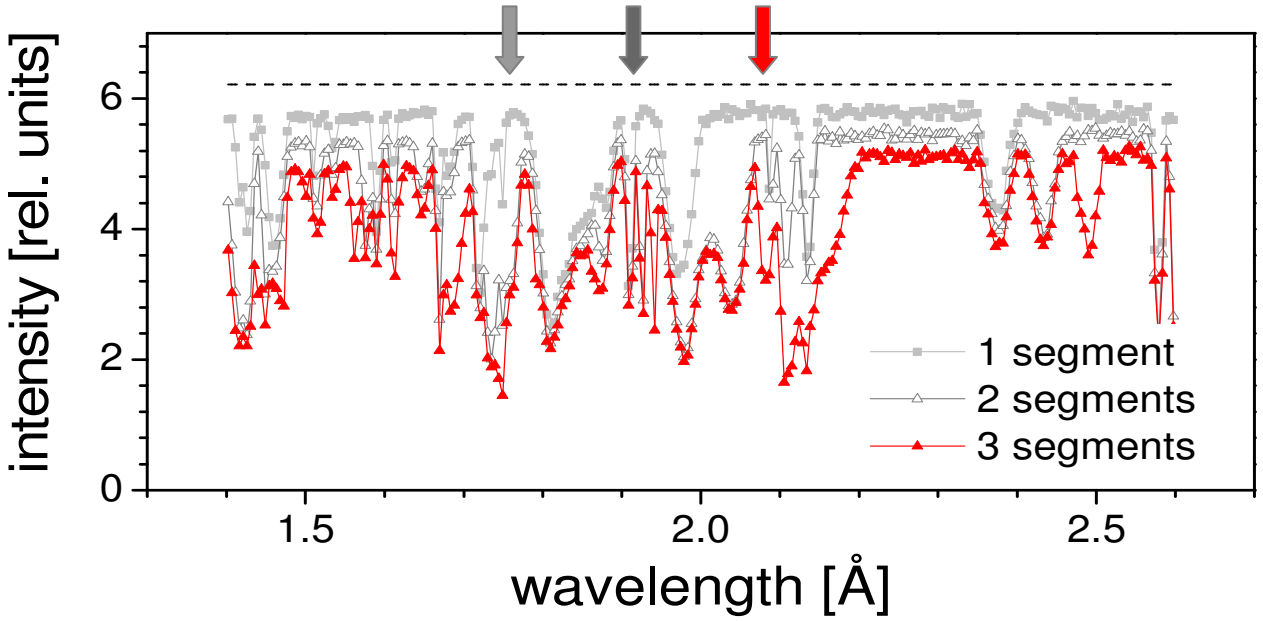

Transmitted spectrum after the 3rd crystal

Search and testing some strong multiple-reflection effects

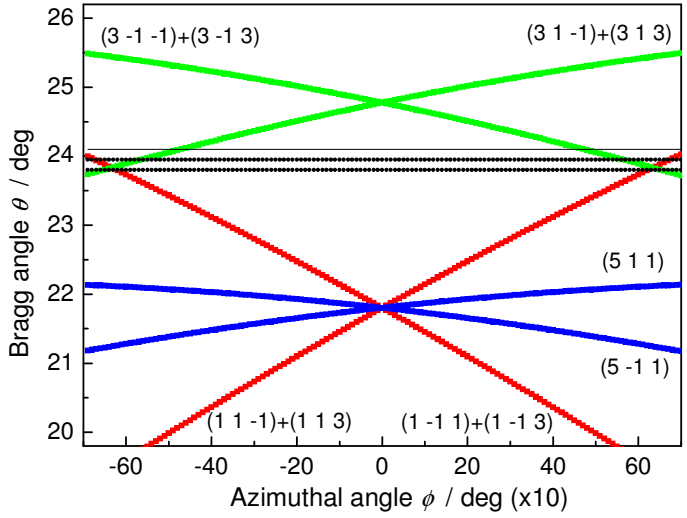

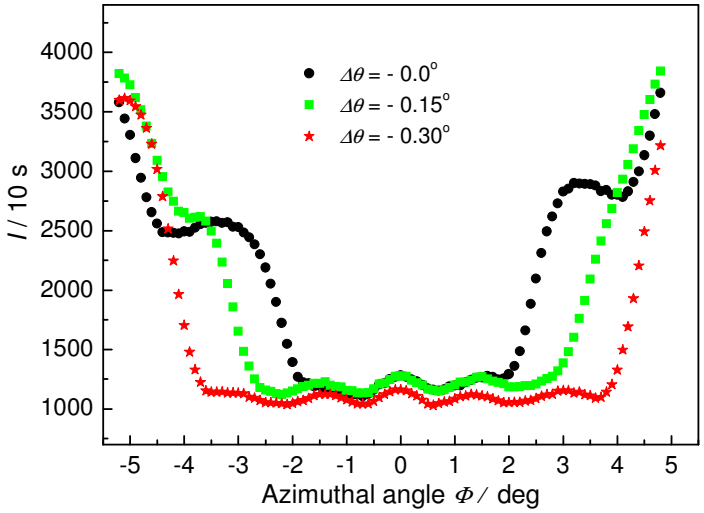

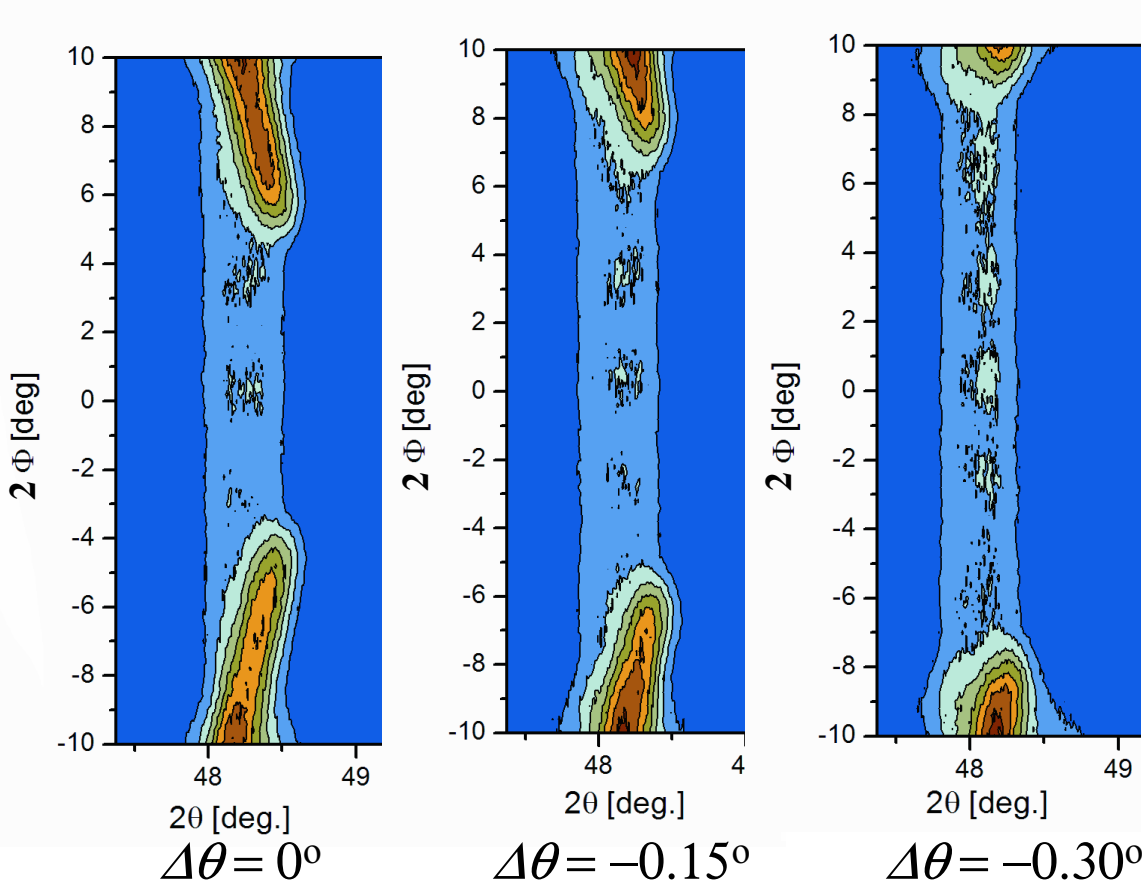

Imaging by PSD detector

Calculated Azimuth-Bragg angle dependences and the experimental results for the crystal Si(002) slabs with the main face parallel to (100). $\lambda = 0.222$ nm.

Search for strong multiple-reflection effects: Azimuthal rotation of the crystal slab for a fixed neutron wavelength

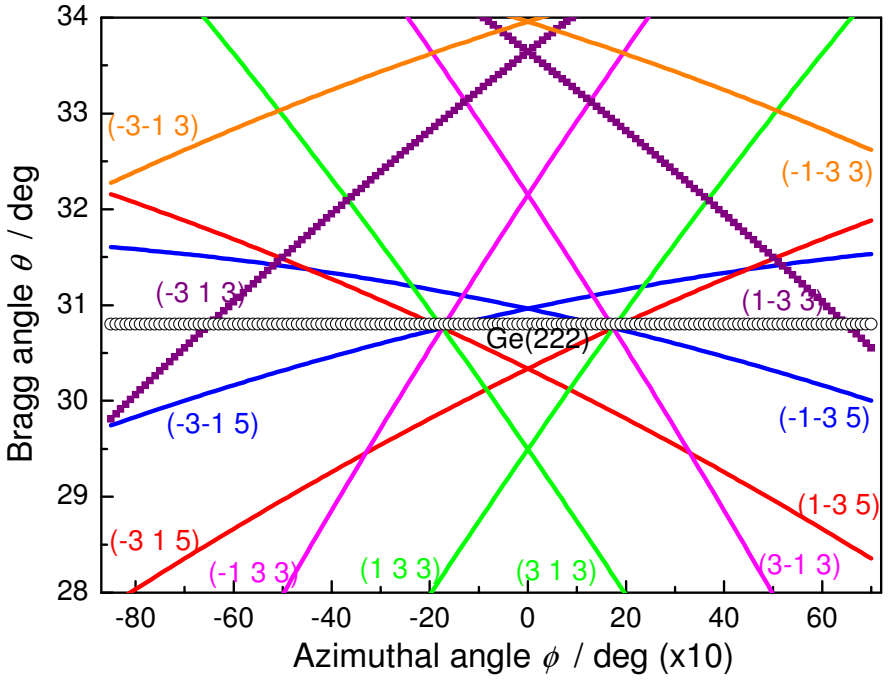

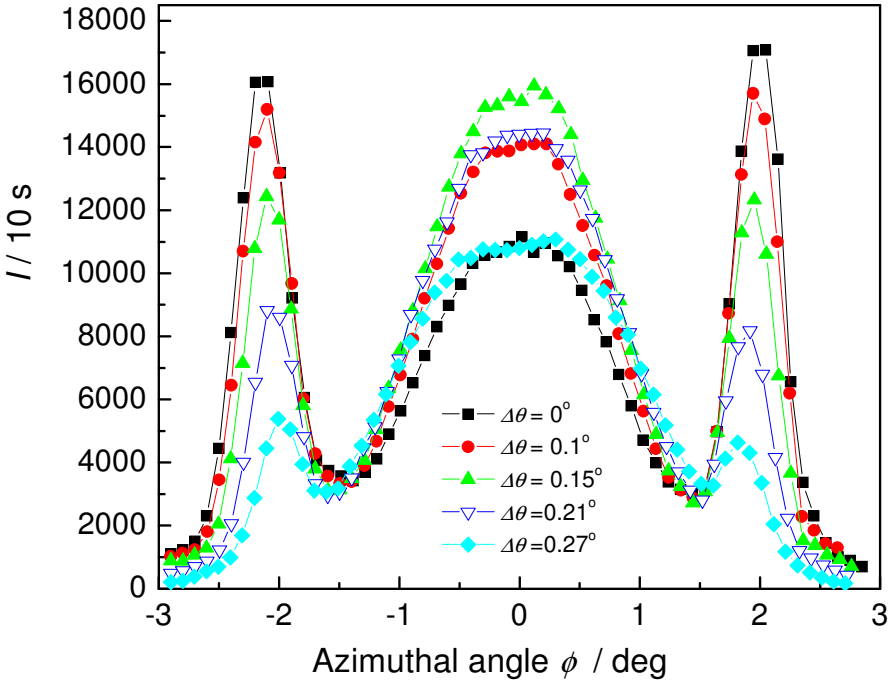

Azimuth-Bragg angle relationship for multiple reflection occurrences related to the 222 reflection in diamond structure. $\Phi = 0^o$ corresponds to the position of the crystal slab with the main face parallel to the 112 planes and perpendicular to the scattering plane. $\theta = 30.8^o$ is the mean Bragg angle for Ge(222) reflection at the fixed wavelength of $\lambda = 0.1657$ nm.

Intensity versus azimuthal angle dependence for Ge(222) bent crystal slab of the thickness of 4 mm and having the main face parallel to the (112) plane for different $\Delta\theta$ from the mean Bragg angle of $\theta = 30.8^o$. Asymmetric transmission geometry, $R = 9$ m.

Set of 7 office staples, λ = 0.165 nm

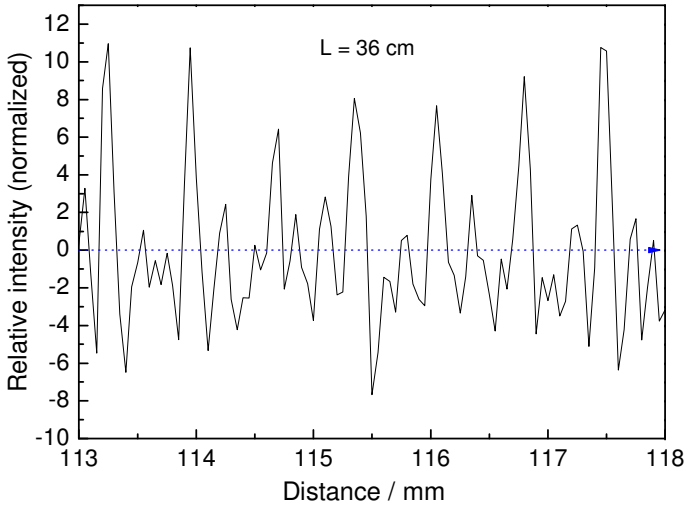

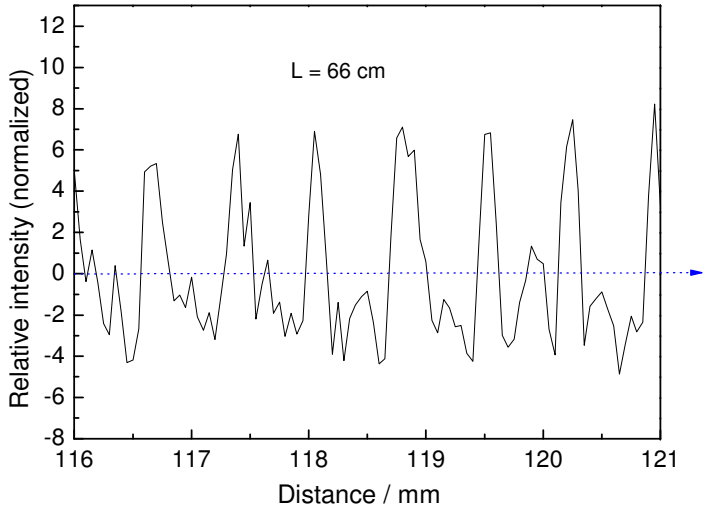

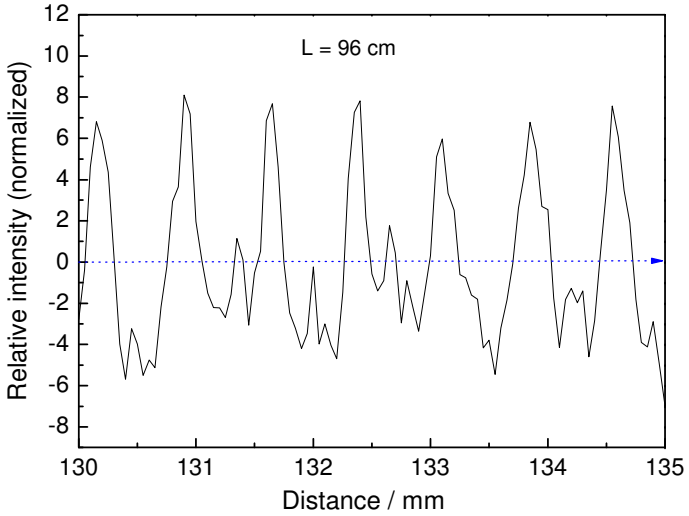

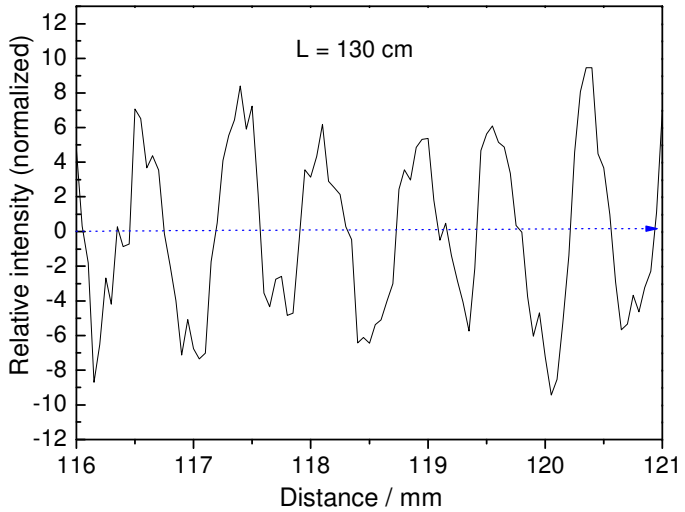

Dependence on the distance of the IP from the sample

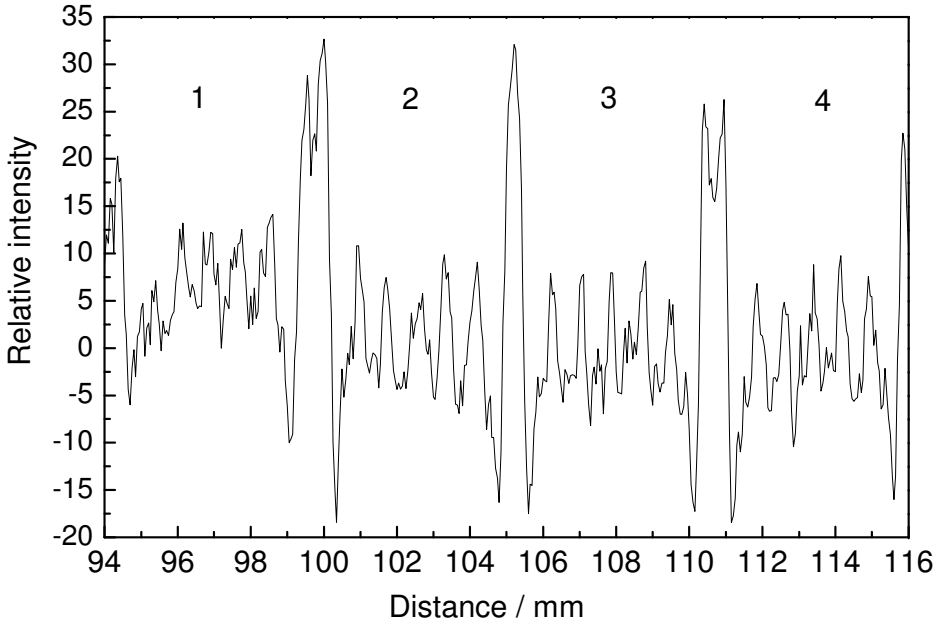

IP at the distance of 50 cm from the sample

4 types of office staples, $\lambda = 0.235$ nm

Properties:

Visibility of the refraction effects depends on the curvature of the MR monochromator

Refraction effects can be observed at the distance of 30 cm from the sample

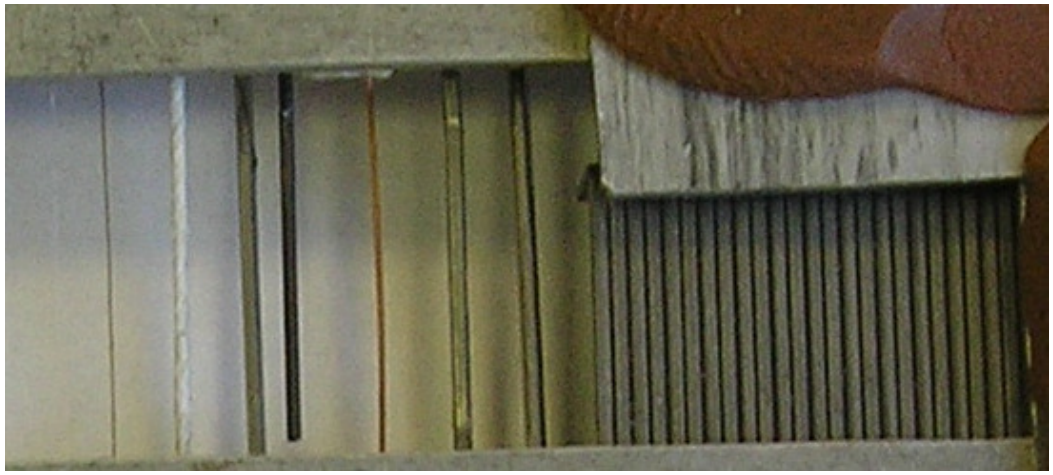

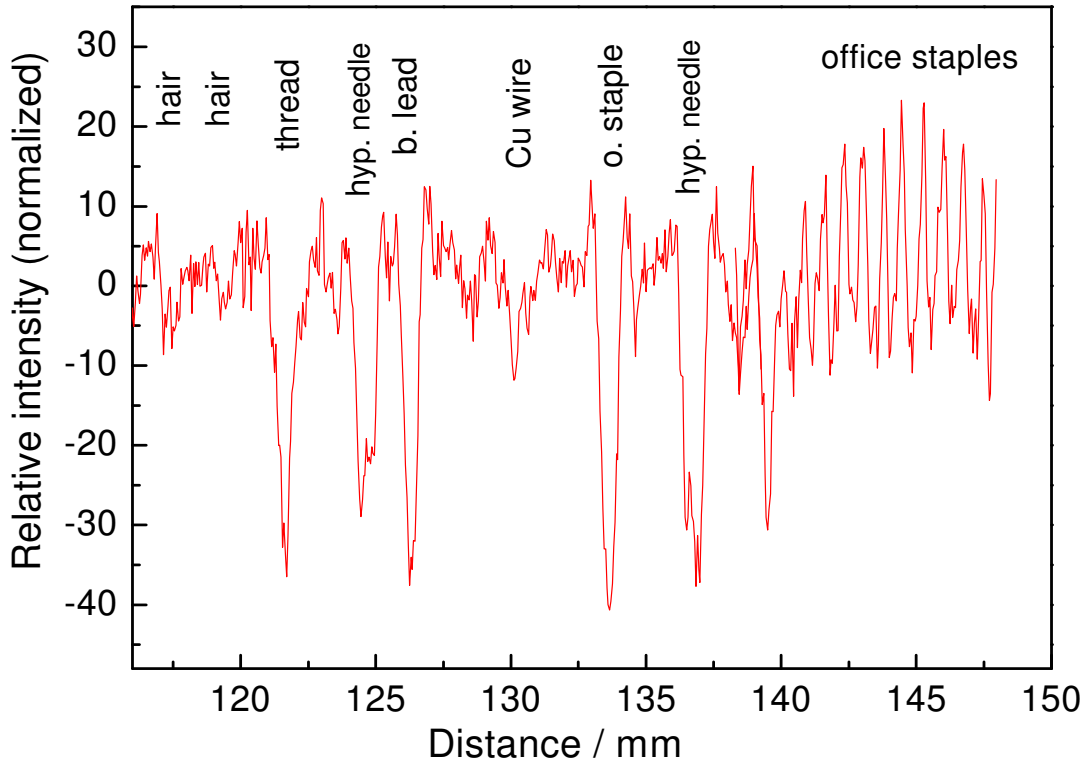

$\lambda = 0.165$ **nm**

Preparations of the search of MR on the neutron optics testing bench

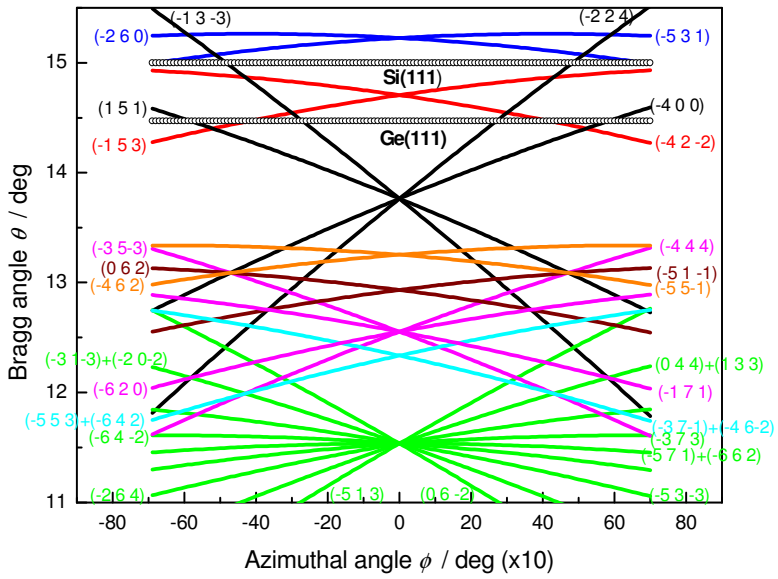

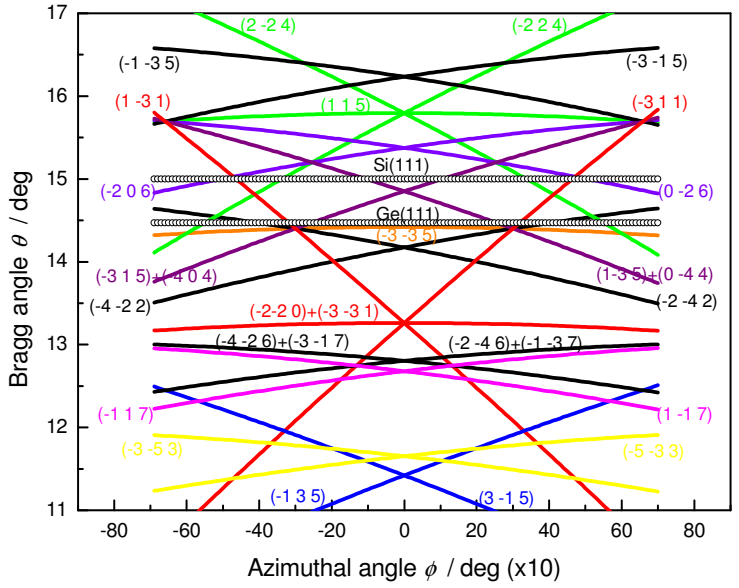

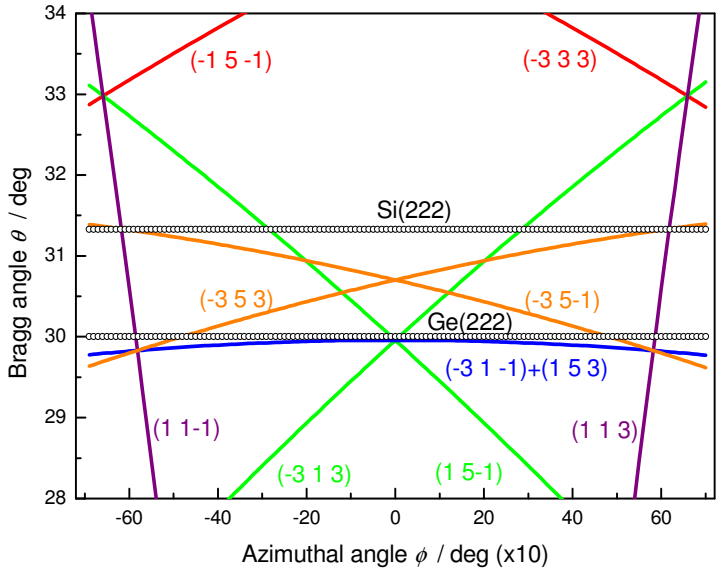

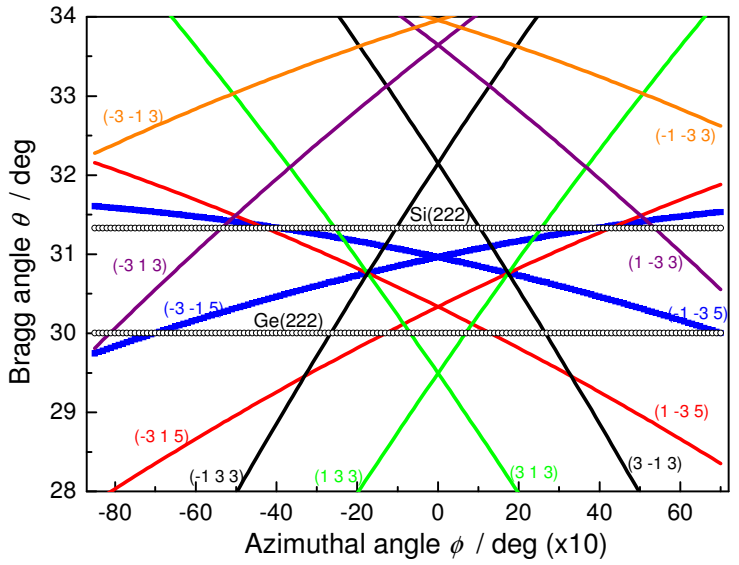

Calculated Azimuth-Bragg angle dependences for the crystal slabs with the main face parallel to (220) and (112) planes, respectively.

Plans

- **Further studies will be carried out on Si(002) - forbidden, Si(004) – allowed, Si(024) – forbidden, Si(424) – forbidden.**
- **Three axis arrangements in combination with PSD will be tested**
- **High resolution radiography studies**
- **High resolution powder diffraction studies**
- **Studies of mosaic distribution of mosaic single crystals**
- **Reflectivity studies of single crystals**

etc.

Sandwich type two crystal dispersive monochromator (continuation)

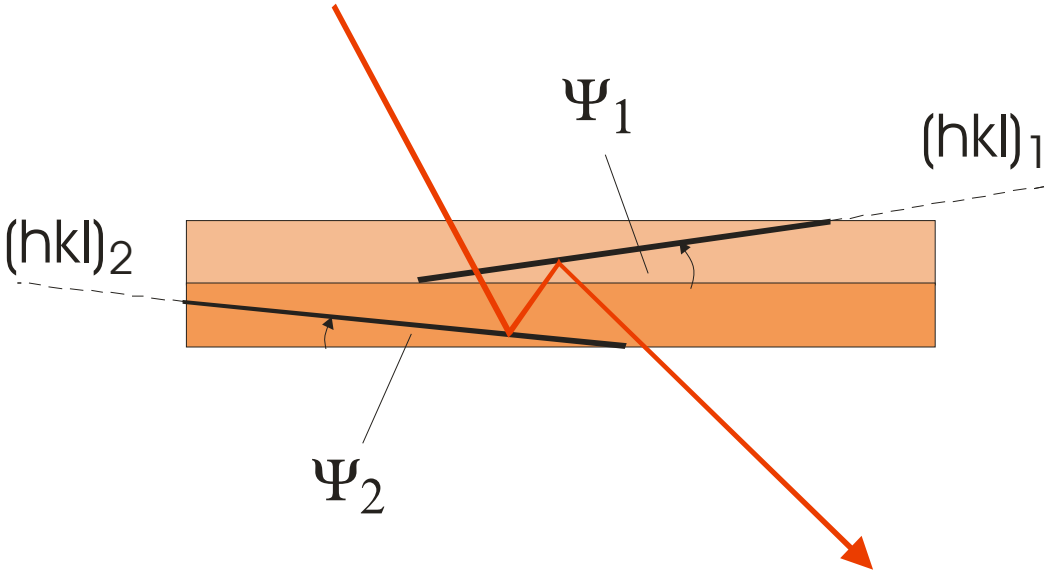

Properties:

Rather small take-off angle

A large Bragg angle (at least) of one reflection

Good peak reflectivity of the bent perfect crystals

Obtained neutron current corresponds to intersection of two corresponding phase-space elements

Possible combinations of bent perfect crystal slabs:

$Si(h_1k_1l_1) + Si\ (h_2k_2l_2)$, $Si(h_1k_1l_1) + Ge(h_2k_2l_2)$. Depending on the cut of the individual crystal slabs many convenient reflection combinations can be found.

Choice of the crystals and reflections

For the preliminary test we used the following combination: The first Si slab had the main face parallel to the planes (1-10) and the longest edge parallel to the vector [111]. The second Si slab had the main face parallel the planes (11-1) and the longest edge parallel to the vector [112].

Si(220) ($\Psi_{220}=0^o$) + Si(331) ($\Psi_{331}=-22.00^o$),	**$\theta_{220}=31.39^o$**	**$\theta_{331}=53.39^o$**	**$\lambda=0.200$ nm**
Si(220) ($\Psi_{220}=0^o$) + Si(4-40) ($\Psi_{440}=-35.23^o$),	**$\theta_{220}=25.99^o$**	**$\theta_{440}=61.22^o$**	**$\lambda=0.168$ nm**
Si(220) ($\Psi_{220}=0^o$) + Si(33$\underline{1}$) ($\Psi_{331}=-48.53^o$),	**$\theta_{220}=40.45^o$**	**$\theta_{331}=88.98^o$**	**$\lambda=0.249$ nm**
Si(311) ($\Psi_{311}=31.48^o$) + Si(333) ($\Psi_{333}=0^o$),	**$\theta_{311}=36.185^o$**	**$\theta_{333}=67.67^o$**	**$\lambda=0.193$ nm**
Si(311) ($\Psi_{311}=-31.48^o$) + Si(33$\underline{1}$) ($\Psi_{331}=-48.53^o$),	**$\theta_{311}=39.30^o$**	**$\theta_{331}=56.35^o$**	**$\lambda=0.207$ nm**
Si(111) ($\Psi_{111}=0^o$) + Si(11-1) ($\Psi_{11-1}=-29.50^o$),	**$\theta_{111}=75.25^o$**		**$\lambda=0.606$ nm**
Si(111) ($\Psi_{111}=0^o$) + Si(11-1) ($\Psi_{11-1}=-29.50^o$),	**$\theta_{111}=14.75^o$**		**$\lambda=0.160$ nm**

Experimental test with the premonochromator

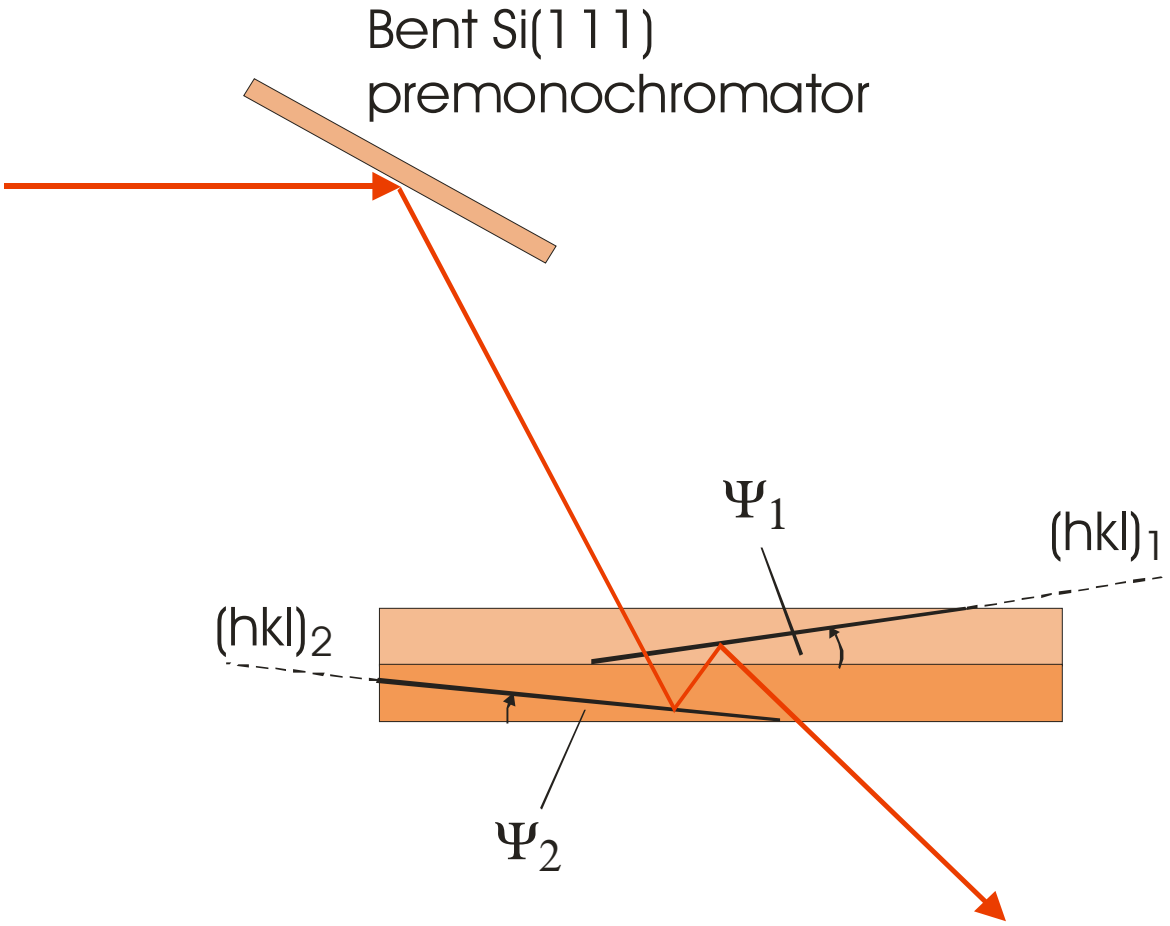

Experimental test with the premonochromator

Si(111) (Ψ_{111}=0°) + Si(11-1) ($\Psi_{11\text{-}1}$=-29.50°)
θ_{111}=75.13° λ=0.606 nm

For the test, λ=0.202 nm and 3rd order reflection was used

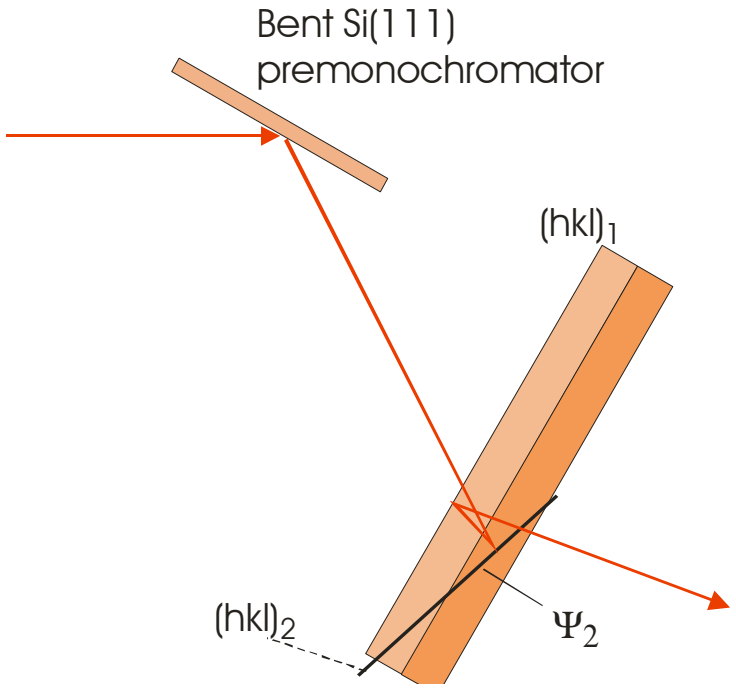

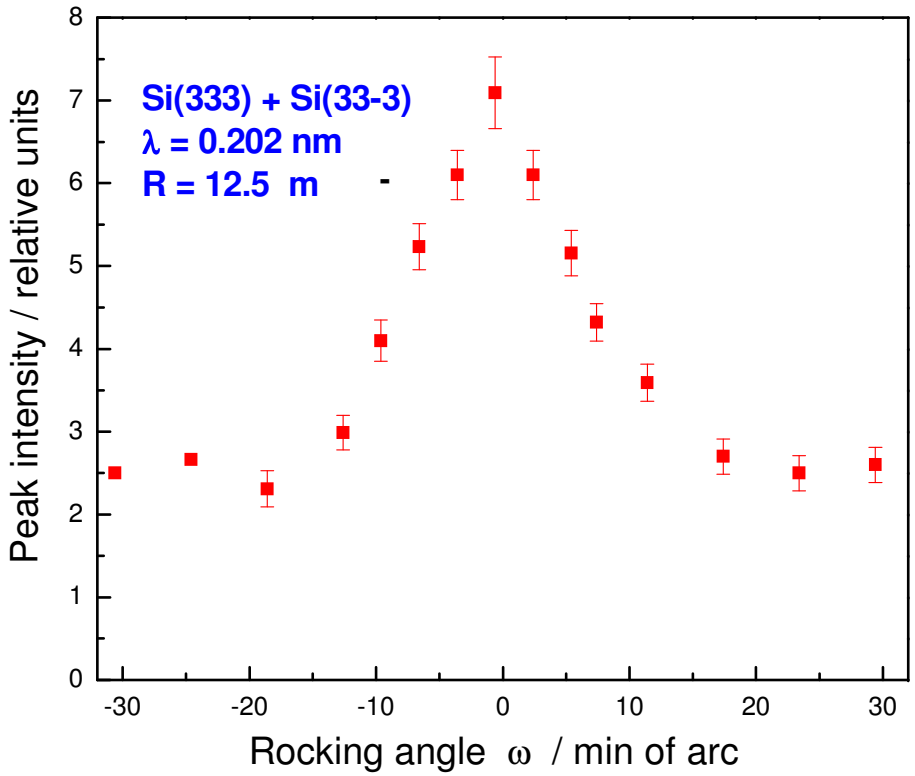

Take-off angle $2\theta_S$=59°

Rocking curve of the sandwich with respect to the premonochromator

Experimental test with the premonochromator

Measurements with higher orders

Si(333) (Ψ_{333}=0º) + Si(33–3) (Ψ_{33-3}=–29.50º

Si(444) (Ψ_{444}=0º) + Si(44–4) (Ψ_{44-4}=–29.50º

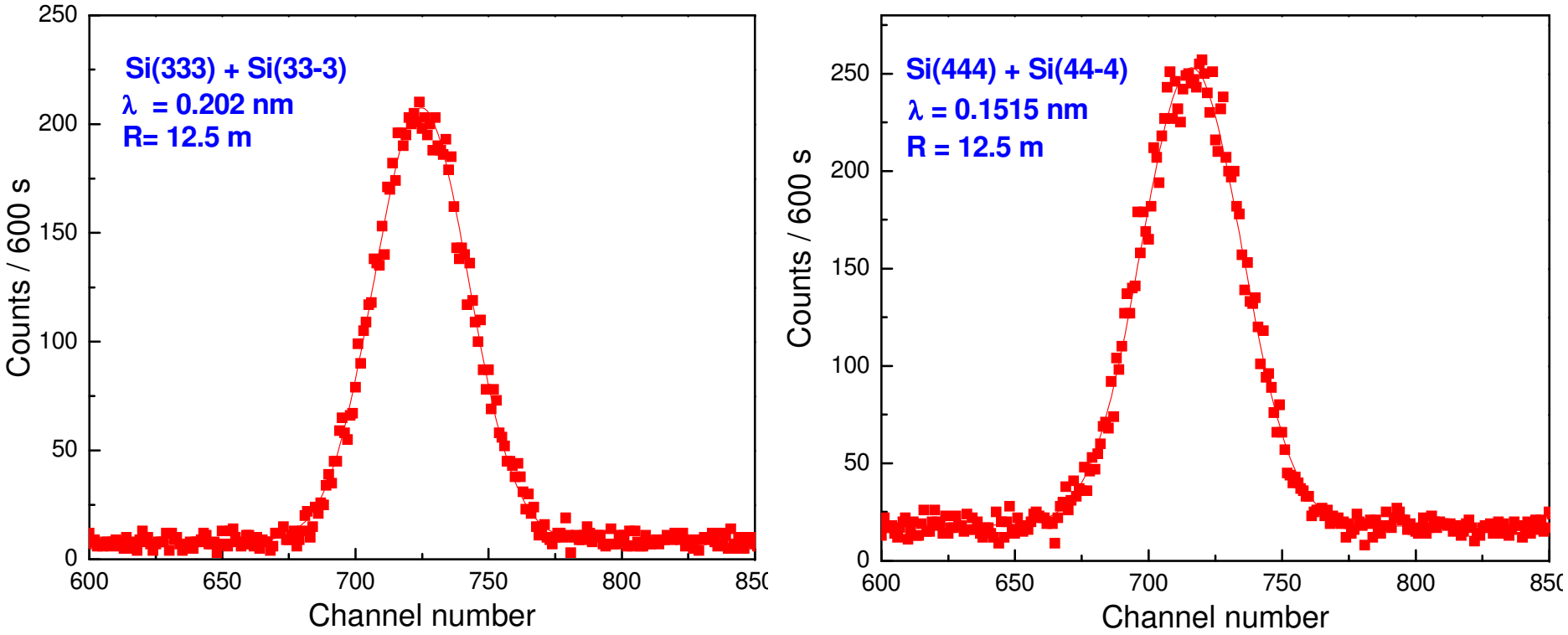

Diffraction profiles as seen by 1d-PSD at the optimum position of the sandwich with respect to the premonochromator

Experimental test with the premonochromator

Take-off angles

Si(220) (Ψ_{220}=0°) + Si(4-40) ($\Psi_{4\text{-}40}$=-35.23°)
θ_{220}=25.99° θ_{440}=61.22° λ=0.168 nm

$2\theta_S$=70.46°

Si(220) (Ψ_{220}=0°) + Si(33-1) ($\Psi_{33\text{-}1}$=-48.53°)
θ_{220}=40.45° $\theta_{33\text{-}1}$=88.98° λ=0.249 nm

$2\theta_S$=97.06°

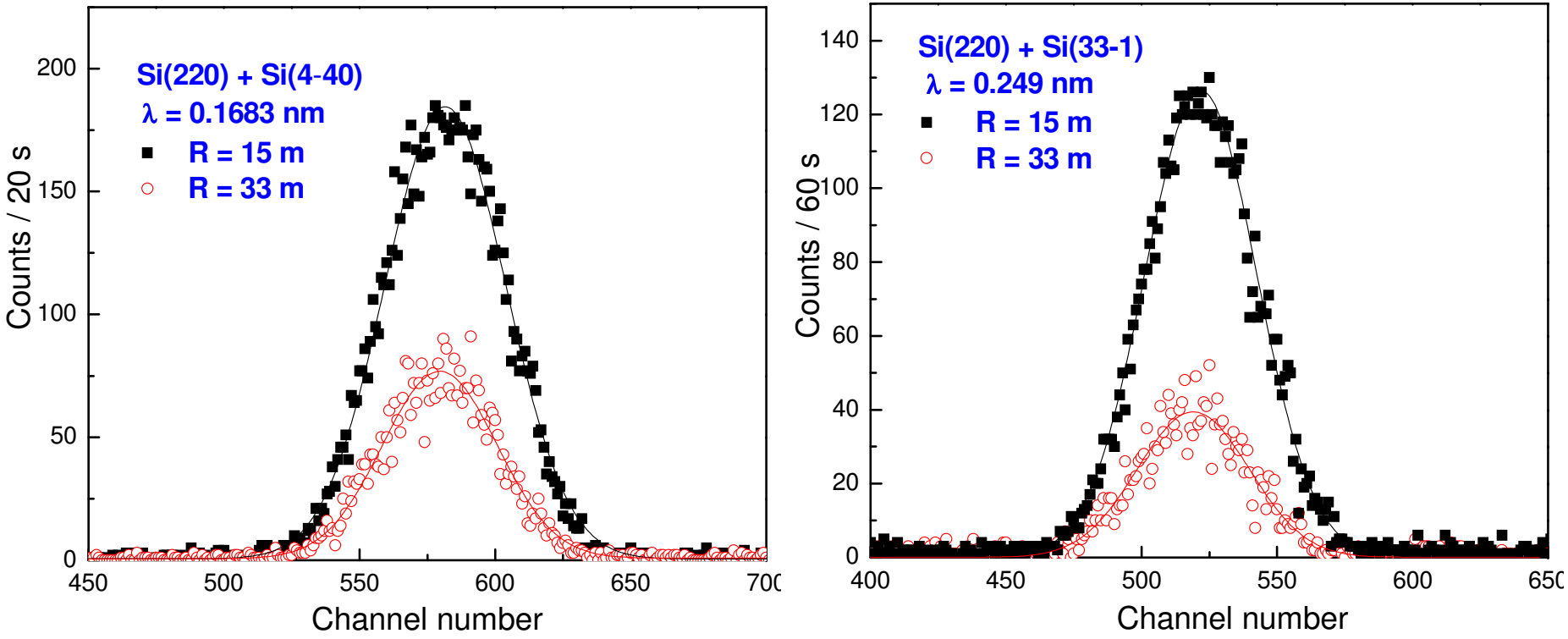

Diffraction profiles as seen by 1d-PSD at the optimum position of the sandwich with respect to the premonochromator